

## Precision diboson observables at the LHC

Marat Freytsis

*Institute for Theoretical Science, University of Oregon,  
Eugene, OR 97403, USA*

In these proceedings, we report on certain ratios of diboson differential cross sections can be used as high-precision observables at the LHC, motivated by the restoration of  $SU(2) \times U(1)$  at high energy. Writing leading-order diboson partonic cross sections in a form that makes their  $SU(2) \times U(1)$  and custodial  $SU(2)$  structure more explicit than in previous literature, identifies important aspects of this structure that survive even in hadronic cross sections. Focusing on higher-order corrections to ratios of  $\gamma\gamma$ ,  $Z\gamma$  and  $ZZ$  processes, we argue that these ratios can be predicted to better than 5%, which should make them useful in searches and characterization of new phenomena. The ratio of  $Z\gamma$  to  $\gamma\gamma$  is especially promising in the near term, due to large rates and to exceptional cancellations of QCD-related uncertainties.

### 1 Introduction

In the Standard Model the electroweak (EW) bosons originate from a triplet and singlet of  $SU(2) \times U(1)$ , becoming massive and mixing after symmetry breaking. But at the high energies accessible to the LHC, the symmetry breaking effects are moderated, and one might imagine the underlying  $SU(2) \times U(1)$  structure might more directly relate diboson processes to one another. It turns out that although this naive expectation is not automatically satisfied, there are nevertheless some elegant and interesting relations.

We identify several independent ratios of diboson measurements that are special at tree level and that offer moderate to excellent potential for both high-precision predictions and high-precision measurements.<sup>1</sup> These ratios, in contrast to the differential cross sections themselves, are flat or slowly-varying as functions of  $p_T$  (and other kinematic variables), making them stable against certain experimental problems. Moreover, many of them receive markedly smaller QCD corrections than the cross-sections themselves, especially at high  $p_T$ .

### 2 Organization at leading order

Well above the scale of EW symmetry breaking, we may rewrite the SM EW bosons  $W^\pm, Z, \gamma$  as the triplet  $w^\pm, w^3$  and singlet  $b$  of massless gauge bosons of  $SU(2) \times U(1)$ , along with the Goldstone scalars  $\phi^\pm, \phi^3$ . Dibosons will receive contributions from varying combinations of  $bb$ ,  $wb$ ,  $ww$ , and  $\phi\phi$  final states. Moreover, the  $ww$  contribution can be further decomposed into an  $SU(2)$  singlet ( $ww_1$ ) and triplet piece ( $ww_3$ ). (A quintet  $ww$  contribution is also possible, for states such as  $W^+W^+$ , but they require two final-state jets, and so will not be considered.) Of the non-Goldstone contribution, only  $ww_3$  receives contributions from the  $s$ -channel,  $f^{abc}$ -proportional contribution, being the only  $SU(2)$ -antisymmetric contribution.

As a result, in the massless limit only three types of amplitudes contribute to all processes:

$$a_1 \propto \mathcal{M}(bb) \propto \mathcal{M}(wb) \propto \mathcal{M}(ww_1), \quad a_3 \propto \mathcal{M}(ww_3), \quad a_\phi \propto \mathcal{M}(\phi\phi). \quad (1)$$

Squared amplitudes relevant for diboson production are then:<sup>2</sup>

$$|a_1|^2 = \frac{\hat{t}}{\hat{u}} + \frac{\hat{u}}{\hat{t}}, \quad |a_3|^2 = \frac{\hat{t}\hat{u}}{4\hat{s}^2} - \frac{1}{8} + \frac{1}{32} \left( \frac{\hat{t}}{\hat{u}} + \frac{\hat{u}}{\hat{t}} \right), \quad (2)$$

$$(a_1 a_3) = \left( \frac{\hat{t} - \hat{u}}{2\hat{s}} \right) + \frac{1}{4} \left( \frac{\hat{t}}{\hat{u}} - \frac{\hat{u}}{\hat{t}} \right), \quad |a_\phi|^2 = \frac{\hat{t}\hat{u}}{4\hat{s}^2}. \quad (3)$$

(( $a_1 a_3$ ) is shorthand for  $\text{Re}(a_1^\star a_3)$ .) The  $a_i$  amplitudes transform simply under  $\hat{t} \leftrightarrow \hat{u}$  exchange:

$$a_1(\hat{t}, \hat{u}) = a_1(\hat{u}, \hat{t}), \quad a_3(\hat{t}, \hat{u}) = -a_3(\hat{u}, \hat{t}), \quad |a_\phi(\hat{t}, \hat{u})| = |a_\phi(\hat{u}, \hat{t})|. \quad (4)$$

These properties of  $a_1$  and  $a_3$ , required by Bose statistics and by the fact that  $ww_1$  ( $ww_3$ ) is symmetric (antisymmetric) in the two  $ws$ , explain why in eqs. (2)–(3) only  $(a_1 a_3)$  is antisymmetric under  $\hat{t} \leftrightarrow \hat{u}$ . These amplitudes allow us to write all the diboson cross-sections in a notation that makes their symmetry properties manifest.

The neutral bosons are produced by various linear combinations of  $bb$ ,  $wb$ , and  $ww_1$ , and so are all proportional to  $|a_1|^2$ . Inserting the appropriate coupling constants and writing  $V^0 = \gamma, Z$ , the partonic cross sections take the form

$$\frac{d\hat{\sigma}}{d\hat{t}}(q\bar{q} \rightarrow V_1^0 V_2^0) = \frac{C_{12}^q}{\hat{s}^2} |a_1|^2, \quad (5)$$

where

$$C_{\gamma\gamma}^q = \frac{1}{2} \frac{\pi \alpha_2^2 s_W^4}{N_c} 2Q^4, \quad C_{Z\gamma}^q = \frac{\pi \alpha_2^2 s_W^2 c_W^2}{N_c} (L^2 Q^2 + R^2 Q^2), \quad C_{ZZ}^q = \frac{1}{2} \frac{\pi \alpha_2^2 c_W^4}{N_c} (L^4 + R^4). \quad (6)$$

Here,  $Q$  is the electric charge of the quark,  $L = T_3 - Y_L t_W^2$ , and  $R = -Y_R t_W^2$  (with  $t_W$  the tangent of the Weinberg angle).

Production of  $W^\pm\gamma$  and  $W^\pm Z$  does involve a  $ww_3$  contribution, with the resulting cross sections being

$$\frac{d\hat{\sigma}}{d\hat{t}}(q\bar{q}' \rightarrow W^\pm\gamma) = \frac{\pi |V_{ud}|^2 \alpha_2^2 s_W^2}{N_c \hat{s}^2} \left[ \frac{Y_L^2}{2} |a_1|^2 \pm 2Y_L(a_1 a_3) + 4|a_3|^2 \right], \quad (7)$$

$$\frac{d\hat{\sigma}}{d\hat{t}}(q\bar{q}' \rightarrow W^\pm Z) = \frac{\pi |V_{ud}|^2 \alpha_2^2}{N_c \hat{s}^2} \left[ \frac{s_W^2 t_W^2 Y_L^2}{2} |a_1|^2 \mp 2s_W^2 Y_L(a_1 a_3) + 4c_W^2 |a_3|^2 + \frac{1}{2} |a_\phi|^2 \right], \quad (8)$$

Because of the smallness of  $Y_L^2 = 1/36$  and the relative factor of  $(8 c_W)^{-1}$  suppressing  $|a_\phi|^2$ , the  $|a_3|^2$  terms naively dominate the cross sections. Conversely, by taking differences of cross-sections with respect to the sign of rapidity difference,  $\text{sign}(\eta_0 - \eta_\pm)$ , of the charged and neutral bosons, all terms except of the  $a_1 a_3$  interference terms can be made to cancel. The  $W^- W^+$  processes can be organized in a similar manner, with analogous statements about anti-symmetrized cross-sections but no clear dominant term in the symmetric ones.

We must make sure that these partonic relations can still be accessed in physical cross-sections after convolution against parton distribution functions (PDFs). This turns out to be the case, even after finite mass effects are included, if cross sections are presented differentially in  $\bar{m}_T$ , the average transverse momentum of the bosons, where  $m_{Ti} = \sqrt{p_{Ti}^2 + m_i^2}$ . Then

$$\frac{d\sigma}{d\bar{m}_T}(pp \rightarrow V_1 V_2) = \sum_{q,q'} \int \frac{d\hat{s}}{s} \int \frac{2\bar{m}_T}{\sqrt{1 - \frac{4\bar{m}_T^2}{\hat{s}}}} \frac{d\hat{\sigma}}{d\hat{t}}(q\bar{q}' \rightarrow V_1 V_2) \int dy f_q(x_1) f_{q'}(x_2), \quad (9)$$

and the integral over PDFs and kinematic variables factorizes. Because of this fact, along with the earlier observation that certain anti-symmetric or symmetric cross sections have very similar kinematic dependences, with only coupling strengths differing, we are naturally lead to consider

ratios of such differential cross-sections. We propose that the following ratios are of interest for their ability to highlight dependence on either particular parameters of the EW sector or PDFs, while suppressing dependence on the other through cancellations between the cross sections:

- $R_{1a} = \frac{\sigma_S(Z\gamma)}{\sigma_S(\gamma\gamma)}$ ,  $R_{1b} = \frac{\sigma_S(ZZ)}{\sigma_S(\gamma\gamma)}$ ,  $R_{1c} = \frac{\sigma_S(ZZ)}{\sigma_S(Z\gamma)}$ ,
- $C_{2a} = \frac{\sigma_S(W^+\gamma)}{\sigma_S(W^-\gamma)}$ ,  $C_{2b} = \frac{\sigma_S(W^+Z)}{\sigma_S(W^-Z)}$ ,  $D_{2a} = \frac{\sigma_A(W^+\gamma)}{\sigma_A(W^-\gamma)}$ ,  $D_{2b} = \frac{\sigma_A(W^+Z)}{\sigma_A(W^-Z)}$ ,
- $R_2^\pm = \frac{\sigma_S(W^\pm Z)}{\sigma_S(W^\pm\gamma)}$ ,  $A_2^\pm = \frac{\sigma_A(W^\pm Z)}{\sigma_A(W^\pm\gamma)}$ ,
- $R_3 = \frac{\sigma_S(W^+W^-)}{\sigma_S(V_1^0V_2^0)}$ ,  $A_3 = \frac{\sigma_A(W^+W^-)}{\sigma_A(WV^0)}$ , (10)

where  $V^0$  denotes  $Z$  or  $\gamma$ , and  $\sigma_A(WV^0)$  is some linear combination of  $\sigma_A(W^+V^0)$  and  $\sigma_A(W^-V^0)$ . Discussions of the specific merits of each ratio are presented in Frye *et al.*<sup>1</sup>

### 3 Higher-order corrections for neutral dibosons

The preceding statements would not be of much use if they only held at leading order, since EW processes at the LHC are known to receive large higher-order corrections. For the simplest of these observables, the  $R_1$  ratios, we have carried out a study of these corrections.

NLO QCD corrections were studied with the help of MCFM.<sup>3</sup> For fixed-order predictions to be reliable, cuts must be chosen carefully beyond leading order to avoid the presence of large logarithms multiplying terms of  $O(\alpha_S)$ , thereby spoiling the reliability of the perturbative expansion.<sup>4</sup> A choice of staggered, sliding cuts makes sure ratios of kinematic variables do not get too large anywhere in accessible phase space:

$$p_T(V_2) > \frac{1}{2} p_T(V_1), \quad H_T = \sum_{\text{jets}} |p_T^j| < \frac{1}{2} p_T(V_2). \quad (11)$$

After defining the cuts in this way, most QCD corrections do cancel in these ratios, except for the region where a final-state jet is collinear with a vector boson. There the photon has a collinear singularity which must be regulated with, *e.g.*, a fragmentation function, while the  $Z$  singularity is regulated by its mass. A naive cone-based isolation procedure introduces a large sensitivity to non-perturbative fragmentation functions that are not very well constrained. This effect can be ameliorated through a “staircase” isolation method,<sup>5</sup> where progressively weaker isolation from hadronic activity is applied at larger angles from the photon, leaving small theoretical uncertainties.

Large corrections are known to occur at NNLO from  $gg \rightarrow V_1^0V_1^0$  contributions. These can shift the ratios by 5–20%, due in part to an accidental cancellation in  $gg \rightarrow Z\gamma$ , but the resulting uncertainties on the shifts are small. Shifts also come from higher-order EW corrections. These can be 5–10%, but the corresponding uncertainty on that value is also small.

These statements are summarized in fig. 1. This plot shows results for  $R_{1a}$ , the ratio of  $Z\gamma$  to  $\gamma\gamma$  cross sections differential in  $\bar{m}_T$ , obtained for the 13 TeV LHC. The upper portion of the plot shows the ratio  $R_{1a}$  as would be measured in 6 bins of 5–6% statistical uncertainty; the last bin includes events with  $\bar{m}_T$  extending up to the kinematic limit. The open circles indicate a LO prediction, while the closed circles are our result including NLO and  $gg$ -initiated production. The dominant corrections are driven by the gluon PDF, and decrease with  $\bar{m}_T$ . The error bars on the closed circles indicate the expected statistical errors at  $300 \text{ fb}^{-1}$ . The shaded band indicates the theoretical uncertainties mentioned in the previous paragraphs, with all uncertainties combined linearly, except for PDF extraction uncertainties which are combined in quadrature with the others. This combination gives a conservative estimate of *known* uncertainties.

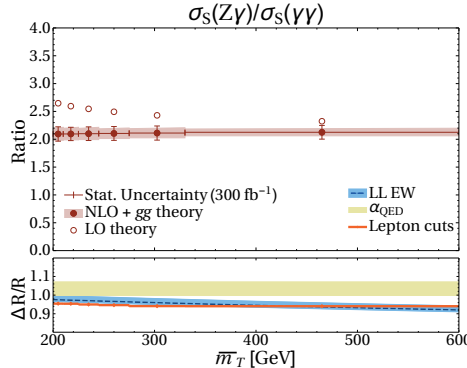


Figure 1 –  $R_{1a}$  with higher-order corrections as described in the text. Projections for experimental uncertainties are also shown for  $300 \text{ fb}^{-1}$  ( $R_{1a}$ ). Analogous results for  $R_{1b}$  and  $R_{1c}$  are presented in Frye *et al.*<sup>1</sup>

#### 4 Conclusions and outlook

We have proposed a wide variety of ratios using LO reasoning about the  $SU(2) \times U(1)$  structure of the SM. We have also shown that for the neutral diboson processes, higher-order corrections do not contradict this reasoning. We are optimistic that a few of the remaining variables will be as precisely predictable as the  $R_1$  ratios. In the meantime, we hope that our methods will inspire invention of other precision observables, perhaps more sophisticated and less obvious, for the LHC and for hadron colliders of the future.

#### Acknowledgments

This work was carried out in collaboration with Christopher Frye, Jakub Scholtz, and Matthew J. Strassler. Support was provided in part by the U.S. Department of Energy grant DE-SC0013607, and National Science Foundation grants PHY-1258729, PHY-0855591, and PHY-1216270.

#### References

1. C. Frye, M. Freytsis, J. Scholtz and M. J. Strassler, JHEP **1603**, 171 (2016) [arXiv:1510.08451 [hep-ph]].
2. R. W. Brown and K. O. Mikaelian, *Phys. Rev. D* **19**, 922 (1979); R. W. Brown, D. Sahdev and K. O. Mikaelian, *Phys. Rev. D* **20**, 1164 (1979); K. O. Mikaelian, M. A. Samuel and D. Sahdev, *Phys. Rev. Lett.* **43**, 746 (1979).
3. J. M. Campbell and R. K. Ellis, *Phys. Rev. D* **60**, 113006 (1999) [hep-ph/9905386]; J. M. Campbell, R. K. Ellis and C. Williams, JHEP **1107**, 018 (2011) [arXiv:1105.0020 [hep-ph]].
4. A. Banfi, G. P. Salam and G. Zanderighi, JHEP **1206**, 159 (2012) [arXiv:1203.5773 [hep-ph]]; A. Banfi, P. F. Monni, G. P. Salam and G. Zanderighi, *Phys. Rev. Lett.* **109**, 202001 (2012) [arXiv:1206.4998 [hep-ph]]; F. J. Tackmann, J. R. Walsh and S. Zuberi, *Phys. Rev. D* **86**, 053011 (2012) [arXiv:1206.4312 [hep-ph]].
5. T. Binoth *et al.* [arXiv:1003.1241 [hep-ph]]; M. Hance, PhD thesis, U. of Pennsylvania, 2011.